Ultrahigh-Resolution STEM Analysis of Complex Compounds

Eiji Abe†, Daisuke Egusa, Ryo Ishikawa, and Takehito Seki

Department of Materials Science & Engineering, University of Tokyo

Aberration-correction of the objective lens has been successful in converging the electron beam into sub-Å scale, and the scanning transmission electron microscopy (STEM) now routinely provides a remarkably improved spatial-resolution both for imaging and spectroscopy. Here we demonstrate the powerful use of the ultrahigh-resolution STEM for the analysis of complex compounds, including long-period modulated and aperiodic quasicrystalline structures.

Introduction

Quantitative determination of local structures, including how dopant elements distribute within the materials, has been one of the challenging issues of electron microscopy. In this regard, scanning transmission electron microscopy (STEM) indeed provided a breakthrough with its significant atomic-number dependent contrast, termed Z-contrast [1], which is able to show up even the single atom embedded in a solid. Besides, STEM enables the spectroscopic analysis at very small scale; local measurements of energy-dispersive x-ray spectroscopy (EDXS) and electron energy loss spectroscopy (EELS) are possible by locating the atomic-sized electron probe on the regions of interest. Owing to recent development of an aberration corrector for the beam-converging lens, STEM is now capable of electron beam with sub-Ångstrom scale, which has remarkably improved its achievable resolution. In this article, we briefly describe some of our recent results to demonstrate the powerful use of the aberration-corrected STEM, which provides immediate insights into the veiled structural/chemical details of the complex compounds.

STEM Experiment

STEM observations were performed by the JEM-ARM200F (Cs-corrected 200 kV STEM/TEM, equipped with a Schottky-emission electron gun) and by the R005 microscope (Cs-corrected 300 kV STEM/TEM, equipped with a (cold) field-emission electron gun). The latter 300 kV-STEM/TEM was developed under a JST-CREST project "Development of the 0.05 nm-Resolution (R005) Electron Microscope" (Leader, Prof. Takayanagi). The minimum full-width half-maximum (FWHM) of the STEM probes are calculated to be approximately ~0.9 Å and ~0.5 Å for 200 kV and 300 kV, respectively. Both STEM indeed provide sub-Ångstrom resolution [2-4], which are demonstrated by imaging the dumbbell atoms separated by less than 1 Å (they occur for the diamond-based structures when viewed along the [112] (or even higher index) direction).

†7-3-1, Hongo, Bunkyo-ku, Tokyo, 113-8656, Japan

E-mail: abe@material.t.u-tokyo.ac.jp

Direct determination of a long-period modulated structure in a $Mg_{97}Zn_1Er_2$ Alloy

Mg alloys containing a small amount of Zn and RE (RE: Y and rare-earth atoms), e.g., $Mg_{97}Zn_1RE_2$ (at.%) alloys reveal excellent mechanical properties with high yield strength over than ~500MPa and elongations better than ~3% at room temperature. One of the key microstructural features is formation of a novel type of long-period ordered (LPO) structure [5], which is long-period chemical-ordered as well as stacking-ordered. There exist several stacking polytypes denoted as 18R, 14H, 10H, 24R, all of which are composed of a common structural unit represented by local ABCA stacking where B- and C-layers are significantly enriched by Zn and RE (these particular layers are denoted as B′- and C′-layers hereafter). It is found that a number of weak satellite spots appear in the diffraction pattern taken along the stacking direction (*c*-axis), suggesting that a further ordering within the close-packed B′- and C′-layers with a six-times modulation along $<\bar{1}2\bar{1}0>\alpha$. Using Cs-corrected STEM, we have investigated the detailed chemical order in the 14H-type LPO structure in the $Mg_{97}Zn_1Er_2$ alloy. Note that Er is a large Z element (Z=68) compared to the others (Mg: Z=12, Zn: Z=30), so that individual Er atoms can be detected through Z-contrast even they are embedded in the complicated structure.

Cs-correction effects appear to be quite significant for the direct imaging of the dense-packed atomic structures, as obviously demonstrated in **Fig. 1** (a) and (b). After Cs-correction, the fundamental reflections of $\bar{1}2\bar{1}0\alpha$ are clearly reproduced in the FFT pattern by accompanying a number of extra weak spots. Concerning that the Z-contrast image reflects a significantly enhanced chemical-potential differences, it can be deduced that the long-period modulation is predominantly due to a concentration modulation along $<\bar{1}2\bar{1}0>\alpha$. To investigate its average features, we construct auto-correlation map from the observed image of Fig. 1(b), and the result is shown in Fig. 1(c). All the atomic sites are successfully reproduced in the auto-correlation map, and the average modulations can be directly derived from the intensity distributions. The short-range Er configurations should be related to the most intense spots in the map, showing that the Er-Er distance is at the second-nearest sites. This is reasonably attributed to a $D0_{19}$-type short-range order, which is in fact frequently observed in the Z-contrast image of Fig. 1(b). By referring further details of the intensity distributions, we are able to construct an average model of the complex long-range modulated structure, as shown in Fig. 1(d).

Local chemistry of a hydrogen-storage $(La, Y)_5Ni_{19}$ complex compounds

$LaNi_X$ ($3 \leq X < 5$) complex compounds with a block-stacking superstructure have attracted increasing attentions due to their reasonably good hydrogen-storage properties at ambient conditions [6,7]. The block-stacking superstruc-

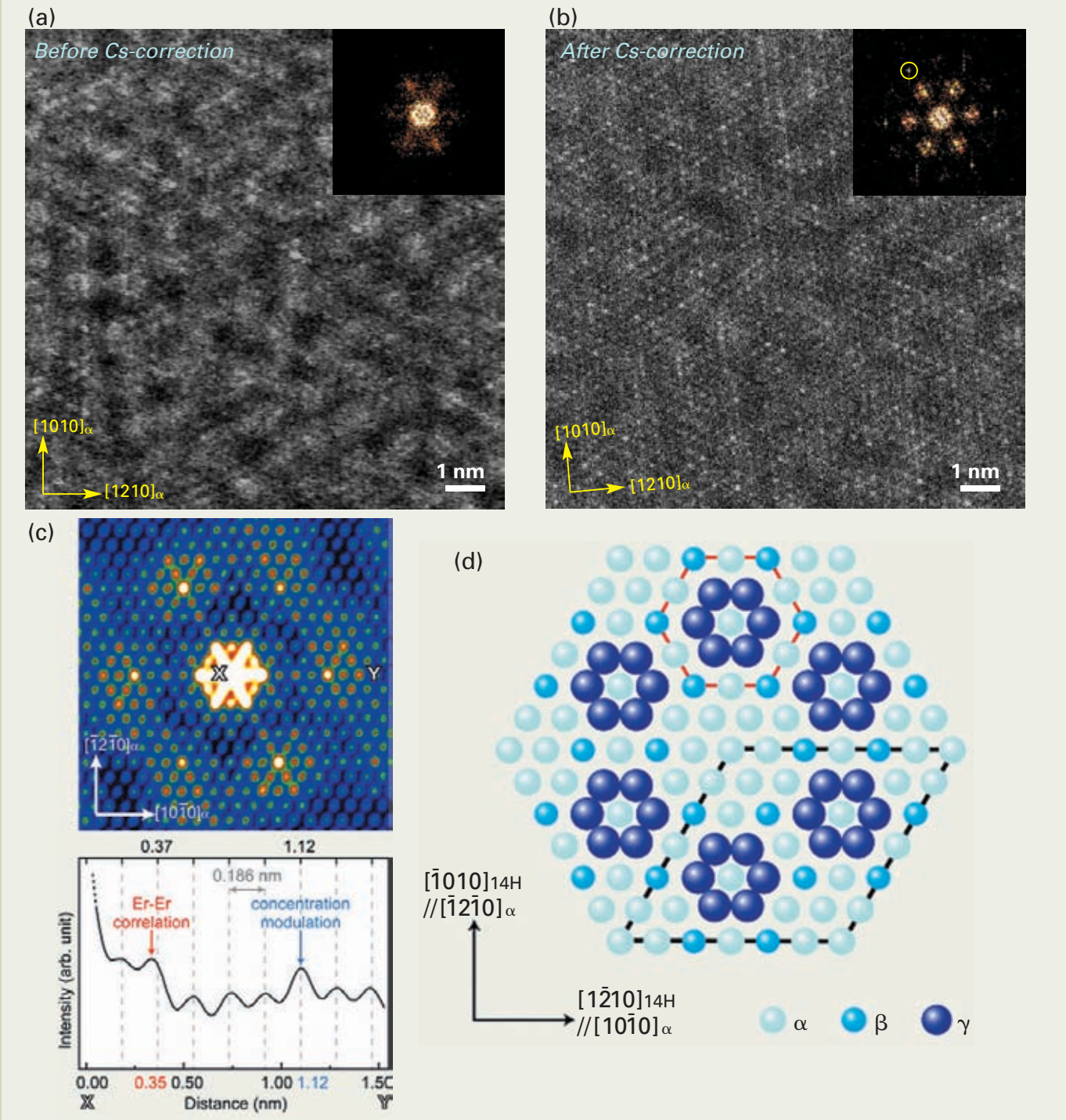

Fig. 1 Atomic-resolution Z-contrast images taken along [0001] axis of the 14H-$Mg_{97}Zn_1Er_2$, obtained with (a) non-Cs-corrected (JEOL JEM-2010F, Cs=0.5mm) and (b) Cs-corrected (JEOL JEM-ARM200F) STEM. (c) Auto-correlation map constructed from the Cs-corrected Z-contrast image of (b). The intensity profile across X-Y is shown below. (d) Average model of the modulated structure, where the composition at the equivalent sites are represented by α, β and γ.

tures are constructed by stacking the "structural blocks", which are represented by Haucke-unit ($LaNi_5$) and Laves-unit ($LaNi_2$). From the previous studies, it is shown that the hydrogen-storage properties of the block-stacking compounds are basically understood by different hydrogenation behaviors of the local Laves-unit/Haucke-unit within the superstructures. For controlling their compositions by the element substitutions to form the (La, X)Ni_χ compounds, it becomes important to understand their favorable substitution sites and how they alter block-unit structures. These local issues are, of course, closely related to the macroscopic hydrogen-storage properties.

Here we describe a change of local chemistry during the hydrogenations of the Y-doped $(La_{0.6}Y_{0.4})_5Ni_{19}$ block-stacking compound. This material is able to store the hydrogen up to ~1.1 H/M (mean number of hydrogen atoms per a constituent-metal atom), but almost the half of the stored-hydrogen will be still retained (~0.5 H/M) even after the discharging process. **Fig. 2** (a) and (b) show the atomic-resolution Z-contrast images of the $(La_{0.6}Y_{0.4})_5Ni_{19}$ compounds, taken from the specimens before and after a hydrogen charge-discharge process. It is clearly seen that an anisotropic lattice expansion along the *c*-axis occurs only at the Laves (L) -unit, as shown by L" in Fig. 2(b), suggesting that the retained-hydrogen are mostly captured in the original L-unit to transform it into the local L" hydrides. In the L" hydride layer, the Ni atoms originally located at the center in the L-unit are found to disappear during the hydrogenations (see the positions indicated by arrowheads in Fig. 2 (a) and (b)), revealing significantly dark Z-contrast as confirmed in the average intensity profiles (Fig. 2(c)). Interestingly, it is also noticed that the profile shows La/Y concentration modulations along the *c*-axis, which have been induced during the hydrogenation process

at room temperature. This is also confirmed by STEM-EDXS, showing significant deficiency/enrichment of Ni/Y at the L″ hydride layer, respectively (Fig. 2(d); note that the Ni concentration seems to modulate along the c-axis, but it could simply due to a delocalization effect. We just draw the conclusion that the local Ni deficiency at the L″ layer is reasonably confirmed by STEM-EDXS with a practical spatial-resolution ~1 nm). Local hydrogen concentration can be successfully evaluated from the shift of the plasmon peaks (ΔE_p) observed between the L and L″ layers (Fig. 2(e)), estimating the possible number of hydrogen atoms to be 7~8 based on a simple free-electron approximation [8,9] and the local composition of the L″ layer as being $(Y,La)_2Ni_3H_8$. This is confirmed to be fairly reasonable values that can account for those determined by the macroscopic chemical analysis. From these systematic analyses by STEM, the change of local chemistry during the hydrogen charge-discharge process is schematically summarized in Fig. 2(f).

Direct determination of a complex quasicrystalline structure $Al_{70}Mn_{17}Pd_{13}$

Quasicrystals are aperiodically long-range ordered solids that exhibit rotational symmetries incompatible with conventional periodic lattice order. Their structure is often described according to a hyperspace crystallography, which interprets the quasicrystal as a periodic structure embedded in a hyperspace. This mathematical recipe enables to calculate the diffraction intensity of any quasicrystal model structures, and accordingly the quasicrystal structures can be, in principle, determined by the x-ray diffraction analysis along the similar manner for periodic crystals.

Al-Mn-Pd alloys form a stable decagonal quasicrystal, a planar realization of the quasi-periodic order. Its structure had been intensively studied by single-quasicrystal X-ray diffraction analysis [10] as well as high-resolution phase-contrast electron microscopy [11,12], which led to the established model structure that reasonably satisfies both the observations.

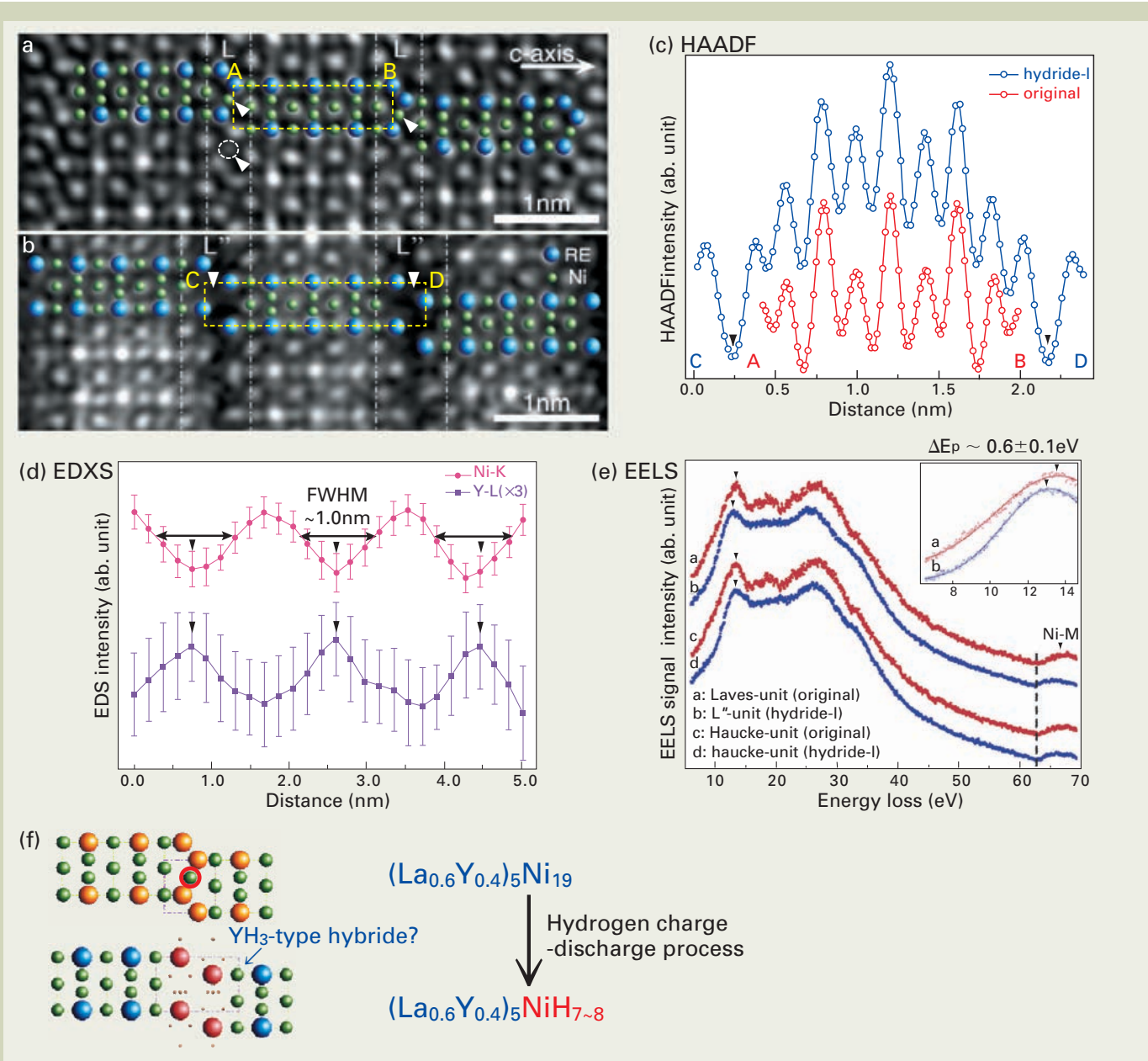

Fig. 2 Atomic-resolution Z-contrast STEM images obtained from the $(La_{0.6}Y_{0.4})_5Ni_{19}$ block-stacking compound; (a) original and (b) after the hydrogenation process. These images are taken by JEOL JEM-ARM200F. (c) HAADF/Z-contrast intensity profiles along the *c*-axis, obtained by integrating over the box regions A-B in (a) and C-D in (b). L″ positions are indicated by the arrowheads. (d) EDX intensity profiles along the c-axis for Ni (red) and Y (blue), where the L" positions are indicated by arrowheads. These are taken using an electron beam with the size of approximately $\phi \sim 3$ Å (current density >~100 pA/cm^2). (d) Low-loss EEL spectra (< 70 eV) obtained from the Laves- and Haucke-units of the original and hydrogenated $(La_{0.6}Y_{0.4})_5Ni_{19}$ compounds, using the smallest electron probe (<~ 1.0 Å). The origins of the spectra positions are corrected by referring the Ni-M edge (68 eV), which appears due to delocalization effects at relatively low-energy regions, even though there is no Ni atoms at the L" layer. Significant peak shift is only observed between the original L- and L″-units, the amount of shift is estimated to be ~ 0.6 ± 0.1 eV after the peak-fitting (inserted). (f) Schematic drawing of the local structural change during the hydrogenation process.

However, the ultrahigh-resolution Z-contrast STEM imaging has unveiled the local details that immediately forces to modify the existing model; see **Fig. 3** (a) and (b). The observed Z-contrast distribution (Fig. 3(a)) cannot be reproduced by the simulation based on the model structure proposed by X-ray analysis [2] (Fig. 3(b)), forcing to modify the local chemical order of Al/Mn/Pd. It should be emphasized here that all the atomic sites, which are densely distributed within the complex quaicrystalline structure and occupied by the atoms of large atomic-number differences (Al: Z=13, Mn: Z=25, Pd: Z=46), are clearly imaged in Fig. 3(a) even under the Z-contrast condition. This demonstrates a remarkable performance of the present 300kV-STEM. As exemplified by the decagonal clusters, the improved structure now fairly well reproduces the observed Z-contrast, as shown in Fig. 3(c). We are now attempting further modifications to describe the entire structure of the decagonal $Al_{70}Mn_{17}Pd_{13}$, with the aid of STEM-EELS to identify details of Mn/Pd occupations at each atomic site. The present results strongly demonstrate again the powerful use of STEM for the study of aperiodcic quasicrystal structures [13-15].

Summary

We have demonstrated the remarkable performance of the state-of-the-art STEM, based on its successful application for elucidations of the multi-component complex structures. At the age of computer-controlled aberration-corrected microscopy, for TEM/STEM experiments special master-hand techniques are not required any longer, and the sub-Å resolution is now routinely and practically available for many types of materials. Given with increasing opportunities for highly quantitative/precise microstructure analysis, we expect that the modern STEM will provide a considerable number of breakthrough results – definitely a new era of microscopic science!

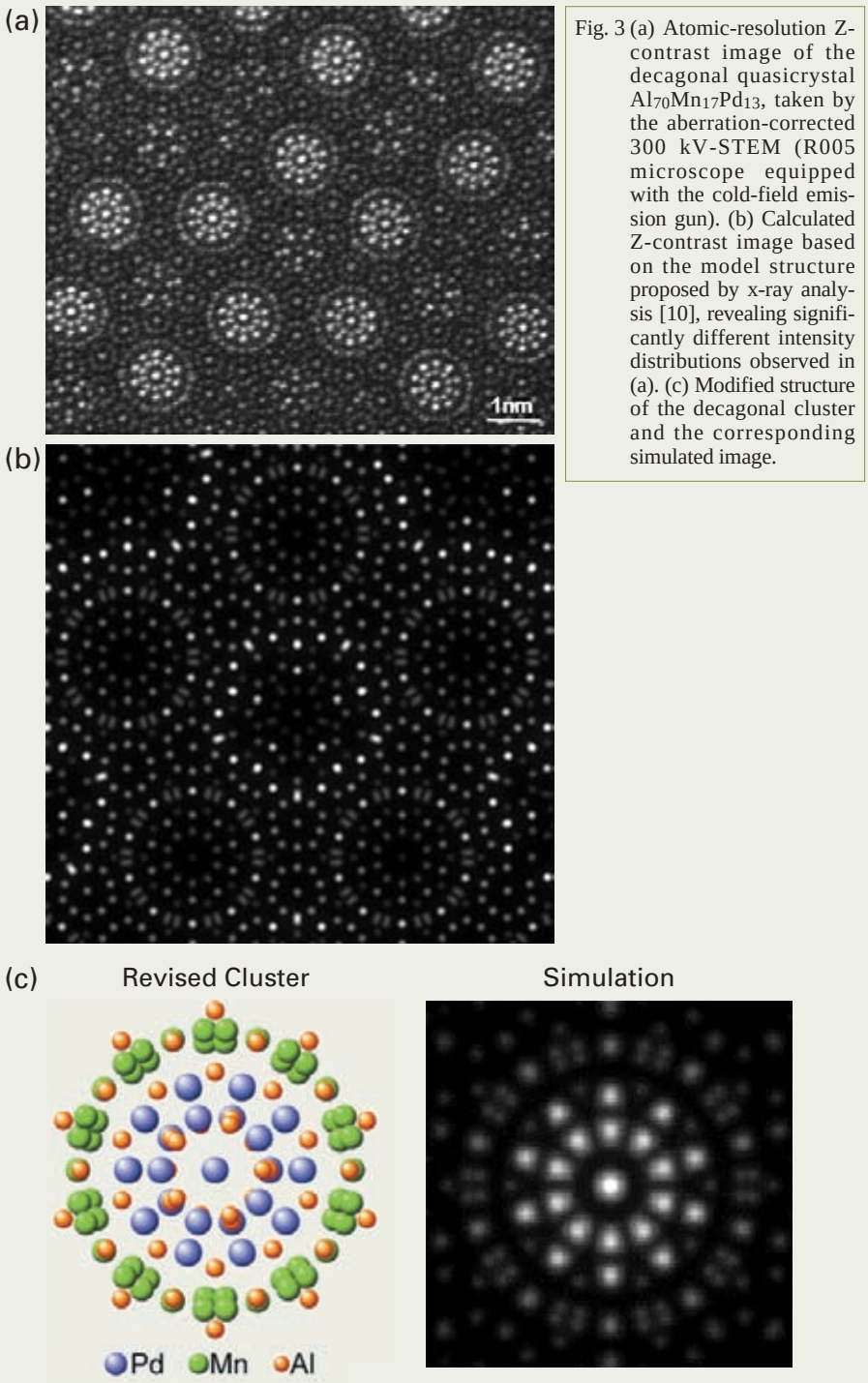

Fig. 3 (a) Atomic-resolution Z-contrast image of the decagonal quasicrystal $Al_{70}Mn_{17}Pd_{13}$, taken by the aberration-corrected 300 kV-STEM (R005 microscope equipped with the cold-field emission gun). (b) Calculated Z-contrast image based on the model structure proposed by x-ray analysis [10], revealing significantly different intensity distributions observed in (a). (c) Modified structure of the decagonal cluster and the corresponding simulated image.

References

[1] S. J. Pennycook, D. E. Jesson, "High-resolution Z-contrast imaging of crystals", *Ultramicroscopy* **37**, 14-38 (1991).

[2] E. Okunishi et al., *Microsc. Microanal.* **15**, (suppl. 2) 164 (2009).

[3] H. Sawada et al., "Achieving 63pm resolution in scanning transmission electron microscope with spherical aberration corrector", *Jpn. J. Appl. Phys.* **46**, L568-L570 (2007).

[4] H. Sawada et al., "STEM imaging of 47-pm-separated atomic columns by a spherical aberration-corrected electron microscope with a 300-kV cold field emission gun" *J. Electron Microscopy* **58**, 357-361, (2009).

[5] E. Abe et al., "Long-period ordered structure in a high-strength nanocrystalline Mg-1at.%Zn-2at.%Y alloy studied by atomic-resolution Z-contrast STEM" *Acta Materialia*, **50**, 3845-3857 (2002).

[6] K. Kadir, T. Sakai, I. Uehara, "Synthesis and structure determination of a new series of hydrogen storage alloys; RMg_2Ni_9 (R=La, Ce, Pr, Nd, Sm and Gd) built from $MgNi_2$ Laves-type layers alternating with AB_5 layers" *J Alloys Compd.* **257**, 115-121 (1997).

[7] T. Kohno et al., "Hydrogen storage properties of new ternary system alloys: La_2MgNi_9, $La_5Mg_2Ni_{23}$, La_3MgNi_{14}" *J Alloys Compd.* **311**, L5-L7 (2000).

[8] R. F. Egerton, *Electron Energy-Loss Spectroscopy in the Electron Microscope*, 2nd Edition, Plenum, New York, 1996.

[9] C. Colliex et al., "Contribution of electron energy loss spectroscopy to the development of analytical electron microscopy" *Ultramicroscopy* **1**, 301-315 (1976).

[10] S.Weber, A.Yamamoto, "Noncentrosymmetric structure of a decagonal $Al_{70}Mn_{17}Pd_{13}$ quasicrystal"*Acta Crystallographica* **A54**, 997 (1998).

[11] K. Hiraga, M. Kaneko, Y. Matsuo, S. Hashimoto, "The structure of Al_3Mn: close relationship to decagonal quasicrystals" *Philosophical Magazine* **B67**, 193-205 (1993).

[12] C. Beeli, S. Horiuchi, "The structure and its reconstruction in the decagonal $Al_{70}Mn_{17}Pd_{13}$ quasicrystal" *Philosophical Magazine* **B70**, 215-240 (1994).

[13] E. Abe, A. P. Tsai, "Structure of quasicrystals studied by atomic-resolution electron microscopy" *JEOL news* **36E**, 18 - 21 (2001).

[14] E. Abe, Y. Yan, S. J. Pennycook, "Quasicrystal as cluster aggregates" *Nature Materials* **3**, 759-767 (2004).

[15] E. Abe,"Structure of Quasicrystals" in *STEM: Imaging and Analysis* (edited by P. Nellist and S. J. Pennycook, Springer, New York, 2010, in press).